

# Exploring the action mechanism of *Oxalis corniculata* L. decoction in treating osteoarthritis utilizing liquid chromatography–mass spectrometry technology combined with network pharmacology

Jian Zhang, MBE<sup>a,b,\*</sup>, Wanyan Shen, BPharm<sup>c</sup>, Hehe He, BPharm<sup>c</sup>

## Abstract

This study aimed to identify the chemical constituents of *Oxalis corniculata* L. decoction. Furthermore, the mechanism of action of *O. corniculata* L. decoction in treating osteoarthritis (OA) was investigated utilizing network pharmacology. The chemical composition of the *O. corniculata* L. decoction was analyzed by employing UHPLC-Q-Exactive-MS/MS. Subsequently, a “compound-target-pathway” network was established through network pharmacology, offering a novel approach to identify the molecular mechanism underlying the treatment of OA with *O. corniculata* L. decoction. Ultimately, the molecular docking technique was employed to validate the binding ability of the active ingredients with therapeutic targets. A total of 539 compounds were identified in *O. corniculata* L. decoction. Topological analysis of the protein–protein interaction network indicated that compounds, including guanosine, naringenin-7-O-beta-D-glucuronide, noroxyhydrastinine, and chrysophanol 8-O-glucoside, have therapeutic potential for OA. In addition, GAPDH, TNF, TP53, epidermal growth factor receptor, and ESR1 may be key targets for the treatment of OA, primarily involving lipid and atherosclerosis, cellular senescence, IL-17 signaling pathway, and epidermal growth factor receptor tyrosine kinase inhibitor resistance signaling pathways. This method preliminarily identified the chemical composition of *O. corniculata* L. decoction and predicted the active ingredients, potential targets, and signaling pathways of *O. corniculata* L. decoction in treating OA. The findings of this research revealed the potential function of *O. corniculata* L. decoction in anti-inflammation, alongside its ability to promote osteoblast proliferation and differentiation, providing new ideas for the processing of *O. corniculata* L. herbs and related drug development.

**Abbreviations:** EGFR = epidermal growth factor receptor, OA = osteoarthritis, PPI = protein–protein interaction.

**Keywords:** network pharmacology, osteoarthritis, *Oxalis corniculata* L. decoction, UHPLC-Q-Exactive-MS/MS

## 1. Introduction

*Oxalis corniculata* L. is a traditional Chinese herbal medicine belonging to the Oxalis family, mainly originating in East Asia.<sup>[1]</sup> It contains flavonoids, steroids, alkaloids, volatile oils, saponins, and other chemical components that exhibit therapeutic properties against inflammation, swelling, and injuries.<sup>[2]</sup> *O. corniculata* L. is currently recognized for its beneficial medicinal properties in the “Quality Standards

of Traditional Chinese and Ethnic Medicinal Materials in Guizhou Province.”<sup>[3]</sup>

Osteoarthritis (OA) is a joint disorder characterized by the progressive degeneration of articular cartilage.<sup>[4]</sup> With prevailing trends of population aging, increasing rates of obesity, and frequent occurrences of traumatic knee injuries, a substantial rise in the incidence and prevalence of OA is expected in the forthcoming decades. In the field of orthopedic treatment, O

This research was funded by the Science and Technology Planning Project of Guizhou Province ([2024]YB091), Guizhou Academy of Agricultural Sciences, Research on Innovation and Efficient Key Technologies of Characteristic Crop Germplasm in Guizhou Hot Zone (Qiannongke Germplasm Resources [2024] No. 08), Guizhou Academy of Agricultural Sciences Youth fund project (QNKYBJJ[2024]10), and Guizhou Provincial Programme to Support High-Quality Creation and Application of Intellectual Property Rights (QZZD[2023]10).

The authors have no conflicts of interest to disclose.

The datasets generated during and/or analyzed during the current study are available from the corresponding author on reasonable request.

Supplemental Digital Content is available for this article.

<sup>a</sup> Guizhou Institute of Subtropical Crops, Guizhou Academy of Agricultural Sciences, Guiyang, China, <sup>b</sup> Key Laboratory of Crop Gene Resources and Germplasm Innovation in Karst, Plateau Mountains, Guiyang, China, <sup>c</sup> Research and Development Department, Guizhou Weikang Zifan Pharmaceutical Co., Ltd., Guiyang, China.

\* Correspondence: Jian Zhang, Guizhou Institute of Subtropical Crops, Guizhou Academy of Agricultural Sciences, Guiyang, Guizhou Province 550000, China (e-mail: nkyzhangjian@163.com).

Copyright © 2024 the Author(s). Published by Wolters Kluwer Health, Inc. This is an open-access article distributed under the terms of the Creative Commons Attribution-Non Commercial License 4.0 (CCBY-NC), where it is permissible to download, share, remix, transform, and buildup the work provided it is properly cited. The work cannot be used commercially without permission from the journal.

How to cite this article: Zhang J, Shen W, He H. Exploring the action mechanism of *Oxalis corniculata* L. decoction in treating osteoarthritis utilizing liquid chromatography–mass spectrometry technology combined with network pharmacology. *Medicine* 2024;103:35(e39515).

Received: 12 March 2024 / Received in final form: 8 August 2024 / Accepted: 9 August 2024

<http://dx.doi.org/10.1097/MD.00000000000039515>

*corniculata* L. has been utilized as its main ingredient in the development of Gukang capsules for OA and osteoporosis, demonstrating its significant therapeutic effects.<sup>[5]</sup> The aqueous extract of *O corniculata* L. can promote the proliferation, differentiation, and mineralization of bone cells *in vitro*<sup>[6]</sup> while also increasing alkaline phosphatase levels, reducing blood viscosity, and improving hemorheology to aid in healing fractures *in vivo*.<sup>[7]</sup> Nonetheless, reports detailing the molecular mechanisms of its medicinal components remain unknown.

In the past few years, network pharmacology has emerged as a popular approach in traditional Chinese medicine. It integrates the principles from systems biology, computer science, and bioinformatics with high-throughput technology to efficiently and economically study the relationship between drugs and diseases.<sup>[8]</sup> This study utilizes UHPLC-Q-Exactive-MS/MS for the analytical profiling of the chemical constituents of *O corniculata* L. decoction and employs network pharmacology coupled with molecular docking techniques to elucidate its mechanisms in treating OA, providing valuable insights for future clinical research and pharmaceutical development.

## 2. Materials and methods

### 2.1. Experimental instruments

The apparatus utilized in this study included an ultra-high performance liquid chromatography–tandem electrostatic field orbitrap mass spectrometer UHPLC-Q Exactive HFX (Thermo Fisher Scientific China Co., Ltd., Shanghai), an Eppendorf 5430R cryogenic high-speed centrifuge (Eppendorf [Shanghai] International Trading Co., Ltd., Shanghai), an SCI-VS vortex mixer (Scilogex, Inc., Rocky Hill, CT), and an SB25-12DTD ultrasonic cleaner (Ningbo Scientz Biotechnology Co., Ltd., Ningbo, Zhejiang).

### 2.2. Reagents

The reagents included crude powder of *O corniculata* L. herb (Guizhou Weikang Zifan Pharmaceutical Co., Ltd., Guizhou city, batch number: YC01-005-20230701), methanol/acetonitrile/formic acid/isopropanol (Anpel, chromatographic grade, Shanghai), 95% ethanol (Shanghai Sangon, Shanghai, analytically pure), and ultrapure water.

### 2.3. Analysis of chemical constituents of *O corniculata* L. decoction

**2.3.1. Sample preparation.** In the first step, 5 g of crude powder of *O corniculata* L. herb was introduced to 150 mL of ultrapure water. Subsequently, the mixture underwent vigorous heating until it reached a boiling point. Following this, it was gently decocted to sustain a mild boil, and the decoction process persisted for a duration of 1 hour. The extract was sieved through a 200-mesh sieve. Afterward, 2 mL of methanol–acetonitrile solution (1:1, v/v) was mixed with 1 mL of supernatant, vortexed for 60 seconds, and sonicated at a low temperature for half an hour. Afterward, the supernatant was isolated by centrifugation at 12,000 rpm and 4 °C for 10 minutes. For protein precipitation, the supernatant was kept at -20 °C for 60 minutes and then centrifuged for 10 minutes at 4 °C and 12,000 rpm. The supernatant was frozen, dried, then redissolved in 100 µL of 50% ACN, vortexed, and centrifuged for 10 minutes at 4 °C and 12,000 rpm. Eventually, the supernatant was collected for analysis.

**2.3.2. Test conditions.** The chromatographic conditions were set as follows: chromatographic column: waters HSS T3 (100 × 2.1 mm, 1.8 µm); column temperature: 40 °C; mobile

phase: 0.1% formic acid–water solution in phase A and 0.1% formic acid–acetonitrile in phase B; flow rate: 0.3 mL/min; elution gradient: 0.0 to 1.0 minutes 0% B, 1.0 to 12.0 minutes 0% → 95% B, 12.0 to 13.0 minutes 95% B, 13.0 to 13.1 minutes 95% → 0% B, and 13.1 to 17.0 minutes 0% B. Throughout the analysis, the sample was maintained in an autosampler at 4 °C, with an injection volume of 2 µL.

The parameters for mass spectrometry were set as follows: Mass spectrometry system: Q Exactive HFX high-resolution mass spectrometry system (Thermo, Branchburg, NJ) employed for the acquisition of primary and secondary spectra. Electrospray ionization conditions: sheath gas flow rate: 40 arb; auxiliary gas flow rate: 10 arb; ion spray voltage: 3000 V/2800 V; temperature: 350 °C; capillary temperature: 320 °C. scanning pattern: full-ms-ddMS2 pattern; scanning mode: positive ion/negative ion; primary scanning range (scan m/z range): 70 to 1050 Da; primary resolution: 70,000; secondary resolution: 17,500.

### 2.4. Network pharmacology

**2.4.1. Acquisition of targets related to *O corniculata* L. decoction.** The structural information of the relevant compounds in the *O corniculata* L. decoction was obtained from NCBI Pubchem (<https://pubchem.ncbi.nlm.nih.gov/>), and their SMILE structural formula was inputted into Swiss Target Prediction (<http://www.swisstargetprediction.ch/>) to acquire targets. Subsequently, the gene names were standardized employing UniProt (<https://www.uniprot.org/>) to attain *O corniculata* L. decoction-related drug targets.

**2.4.2. OA-related target acquisition and protein–protein interaction (PPI) network construction.** By using the keyword ‘osteoarthritis’, OA-related genes were retrieved from 3 disease gene databases, including GeneCards (<https://www.genecards.org/>), CTD Database (<https://ctdbase.org/>), and DisGeNET Database (<https://www.disgenet.org/>). Subsequently, the data retrieved in the 3 databases were aligned and de-duplicated to obtain disease-related targets.

The component targets of *O corniculata* L. decoction were intersected with OA targets utilizing the online software Venny (<https://bioinfogp.cnb.csic.es/tools/venny/>). The common targets of the 2 represent the potential targets of *O corniculata* L. decoction in treating OA. The intersected targets were imported to the STRING, with the screening criterion set at a minimum required interaction score of ≥0.4. Furthermore, the PPI network diagram and TSV format file were downloaded and saved. Ultimately, Cytoscape 3.9.0 was employed to visualize the PPI network to construct a multidimensional network diagram representing the “drug component–target–pathway.”

**2.4.3. GO functional enrichment and KEGG pathway enrichment analyses.** GO and KEGG enrichment analyses of the core targets were conducted by employing R language software to explore the possible biological functions and major signaling pathways of *O corniculata* L. in treating OA. The enrichment analysis outcomes with significant differences were filtered by descending order as per the *P*-value with *q* value < 0.05 as the criterion. Ultimately, the enrichment results yielded the GO biological functions and the top 20 KEGG signaling pathways.

**2.4.4. Molecular docking.** The targets with the top 5 degree values in the PPI network were selected as the key potential action targets for the treatment of OA. Subsequently, these targets were molecularly docked with the core active ingredients exhibiting top 5 degree values. The protein structures of the core targets within the intersecting targets were retrieved from the RCSB database in the PDB format, while the compound

structures were obtained from PubChem. The target proteins and small molecule compounds were preprocessed utilizing AutoDock software, followed by format conversion and analysis of protein binding sites to identify the corresponding docking activity pockets. The target proteins and small molecule compounds were imported into AutoDock Vina 1.1.2 docking software, and the coordinates of docking sites were set for docking verification. Finally, PyMol software was utilized for the visualization of core targets.

### 3. Results

#### 3.1. Identifying the chemical components of the *O. corniculata* L. decoction

A total of 539 compounds were identified in the *O. corniculata* L. decoction (Table S1, Supplemental Digital Content, <http://links.lww.com/MD/N478>), of which 315 were detected in positive ion mode and 224 in negative ion (Fig. 1). Classification analysis of the compounds revealed 86 flavonoids, 64 organo-oxygen compounds, 52 prenol lipids, 36 carboxylic acids and derivatives, 26 fatty acyls, 21 benzene and substituted derivatives, 21 coumarins and derivatives, 16 cinnamic acids and derivatives, 16 isoflavonoids, 10 benzopyrans, 10 phenols, 8 purine nucleosides, 7 anthracenes, 7 diarylheptanoids, and 160 other compounds.

The top 30 compounds in the *O. corniculata* L. decoction were selected based on the relative peak area for network pharmacological analysis (Table 1). A total of 252 targets corresponding to the 30 components were obtained from the Swiss Target Prediction database. Additionally, 4891, 6497, and 368 OA-related targets were retrieved from GeneCards, CTD, and DisGeNET disease databases, respectively. Further intersection with drug target genes yielded 190 potential targets that may be associated with OA treatment (Fig. 2).

#### 3.2. Protein-protein interaction (PPI) network

The 190 intersecting targets with OA were imported into the STRING database to elucidate the interactions between component targets. Further, 190 proteins and 1621 interaction links were obtained. The obtained PPI information was imported into Cytoscape for visualization and analysis. The PPI network is shown in Figure 3. Subsequently, the screening of 35 core targets was conducted as per the definition of higher-than-average values of degree, betweenness centrality, and closeness centrality (Table S2, Supplemental Digital Content, <http://links.lww.com/MD/N479>). The top 10 targets in terms of degree values were GAPDH, TNF, TP53, epidermal growth factor receptor (EGFR), ESR1, PTGS2, MMP9, CXCL8, CCND1, and GSK3B (Table 2). This finding suggests that the compounds present in *O. corniculata* L. decoction

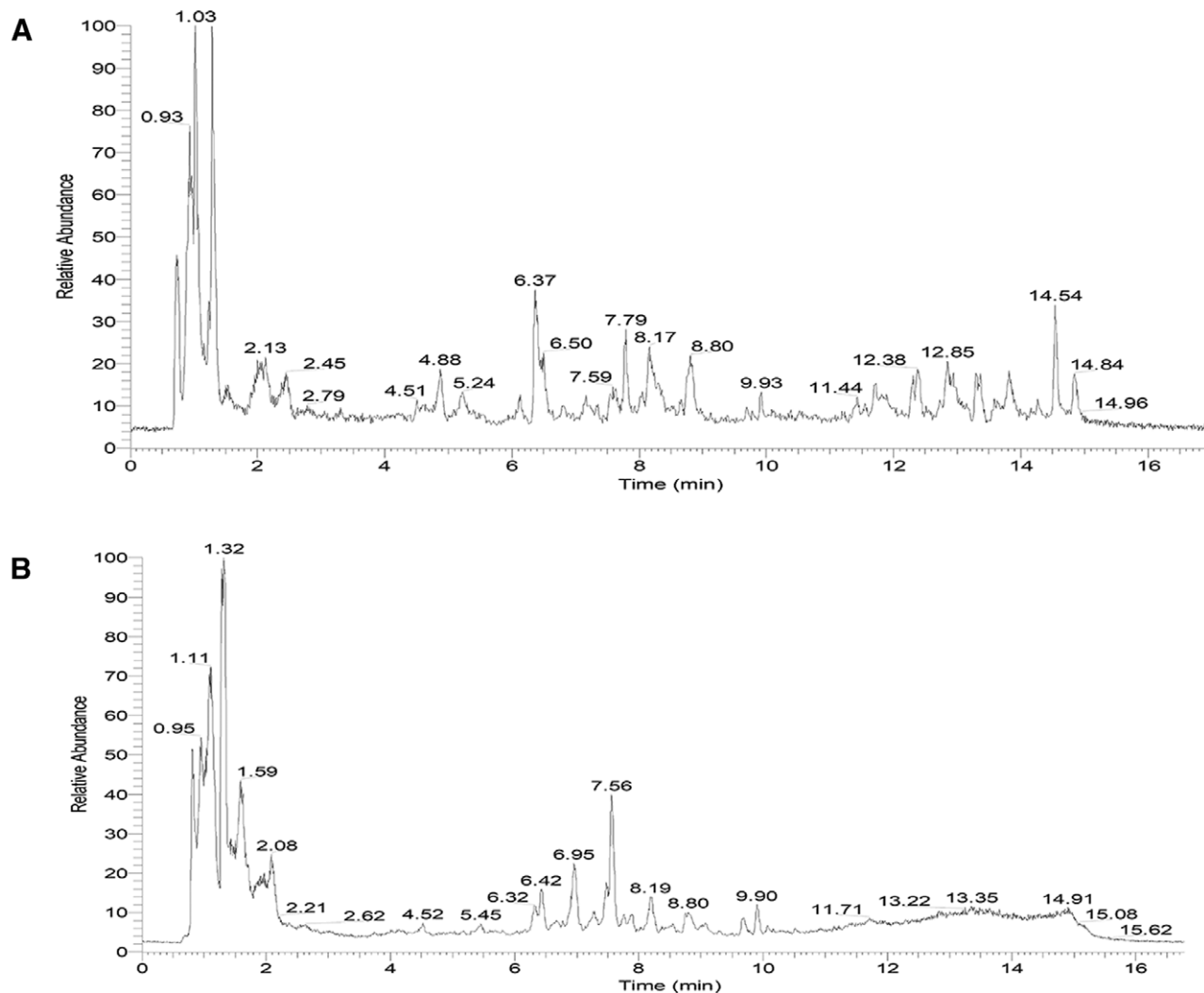


Figure 1. TIC diagram of positive ion (A) and negative ion (B) mode of *Oxalis corniculata* L. decoction.

Table 1

The relative content of the top 30 compounds in *Oxalis corniculata* L. water decoction.

No.	Compound	Formula	Rt (minutes)	m/z	Ion mode	Pubchem ID
1	D-proline	C <sub>5</sub> H <sub>9</sub> NO <sub>2</sub>	1.03	116.070842	POS	8988
2	3'-hydroxy puerarin	C <sub>21</sub> H <sub>20</sub> O <sub>10</sub>	8.75	433.112201	POS	5748205
3	Naringenin-7-O-beta-D-glucuronide	C <sub>21</sub> H <sub>20</sub> O <sub>11</sub>	8.23	449.107011	POS	15540754
4	10-O-Coumaroyl-10-O-deacetylasperuloside	C <sub>25</sub> H <sub>26</sub> O <sub>12</sub>	8.04	563.140250	NEG	95224286
5	Isoorientin	C <sub>21</sub> H <sub>20</sub> O <sub>11</sub>	8.23	447.092922	NEG	114776
6	Isoschaftoside	C <sub>26</sub> H <sub>26</sub> O <sub>14</sub>	8.54	563.140260	NEG	3084995
7	Isovitexin	C <sub>21</sub> H <sub>20</sub> O <sub>10</sub>	8.75	431.097826	NEG	162350
8	Kaempferol 3-glucoside 7-rhamnoside	C <sub>27</sub> H <sub>30</sub> O <sub>15</sub>	7.60	595.164946	POS	57390614
9	4''-Methoxy-genistin	C <sub>22</sub> H <sub>22</sub> O <sub>10</sub>	8.82	445.113525	NEG	71621984
10	Emodin-8-O-beta-gentiobioside	C <sub>27</sub> H <sub>30</sub> O <sub>15</sub>	7.60	593.151005	NEG	71587230
11	Betaine	C <sub>5</sub> H <sub>11</sub> NO <sub>2</sub>	0.94	118.086448	POS	247
12	Ruberythric acid	C <sub>25</sub> H <sub>26</sub> O <sub>13</sub>	7.72	579.135219	NEG	92101
13	Panasenoside	C <sub>27</sub> H <sub>30</sub> O <sub>16</sub>	7.24	611.159852	POS	9986191
14	N-acetyl-neuraminic acid	C <sub>11</sub> H <sub>19</sub> NO <sub>9</sub>	1.67	290.087725	NEG	439197
15	Neoschaftoside	C <sub>26</sub> H <sub>26</sub> O <sub>14</sub>	7.72	563.140295	NEG	442619
16	2-Oxo-3-phenylpropanoic acid	C <sub>9</sub> H <sub>8</sub> O <sub>3</sub>	6.51	147.043935	POS	997
17	Trigonelline	C <sub>7</sub> H <sub>9</sub> NO <sub>2</sub>	1.01	138.054910	POS	5570
18	N-a-Acetyl-L-arginine	C <sub>8</sub> H <sub>16</sub> N <sub>4</sub> O <sub>3</sub>	1.30	280.138480	POS	67427
19	4-Aminobutyric acid	C <sub>4</sub> H <sub>9</sub> NO <sub>2</sub>	0.94	104.071033	POS	119
20	3-Methyladipic acid	C <sub>7</sub> H <sub>12</sub> O <sub>4</sub>	6.34	205.071081	NEG	12292
21	Adenine	C <sub>5</sub> H <sub>4</sub> N <sub>5</sub>	1.30	136.061779	POS	190
22	Verproside	C <sub>22</sub> H <sub>26</sub> O <sub>13</sub>	8.85	463.122502	POS	12000799
23	(-)-Epicatechin	C <sub>15</sub> H <sub>14</sub> O <sub>6</sub>	6.45	291.085685	POS	72276
24	Chrysophanol 8-O-glucoside	C <sub>21</sub> H <sub>20</sub> O <sub>9</sub>	8.85	461.108527	NEG	442731
25	Opuntiol	C <sub>7</sub> H <sub>8</sub> O <sub>3</sub>	1.06	174.075959	POS	10034839
26	D-Leucine	C <sub>6</sub> H <sub>13</sub> NO <sub>2</sub>	2.01	132.101923	POS	439524
27	Noroxxyhydrastinine	C <sub>10</sub> H <sub>9</sub> NO <sub>3</sub>	7.58	236.055963	NEG	89047
28	myo-Inositol	C <sub>6</sub> H <sub>12</sub> O <sub>6</sub>	1.06	179.055203	NEG	892
29	Rubrofusarin-6-O-beta-D-gentiobioside	C <sub>27</sub> H <sub>32</sub> O <sub>15</sub>	8.71	577.155950	NEG	503733
30	Guanosine	C <sub>10</sub> H <sub>13</sub> N <sub>5</sub> O <sub>5</sub>	2.05	284.098334	POS	135398635

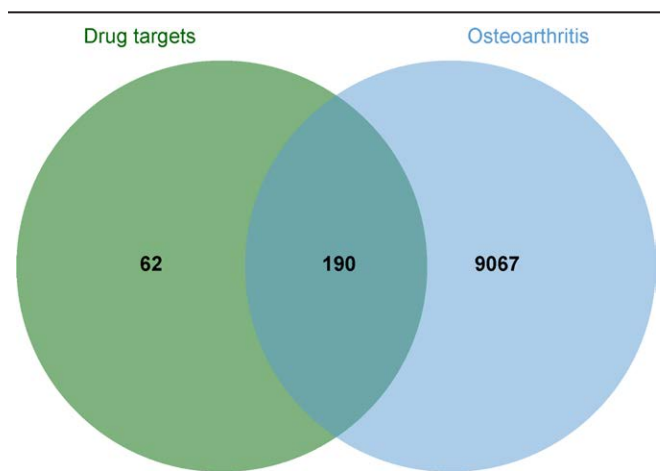


Figure 2. Intersection mapping of component targets of *Oxalis corniculata* L. decoction with OA targets. OA = osteoarthritis.

may primarily act on these core targets to exert pharmacological effects on OA.

### 3.3. GO and KEGG enrichment analyses

The GO enrichment analysis of 190 potential targets was conducted by utilizing the “Cluster Profiler” package in R language, yielding a total of 2443 items. Among them, 2178 items were enriched in the biological process category, primarily including response to xenobiotic stimulus, regulation of inflammatory response, neuron death, regulation of trans-synaptic signaling, and regulation of neuron death. Moreover, 172 items were enriched in the molecular function category, primarily including

serine hydrolase activity, serine-type peptidase activity, steroid binding, endopeptidase activity, and nuclear receptor activity. Additionally, 93 items were enriched in the cellular component category, primarily involving membrane raft, membrane microdomain, postsynaptic membrane, glutamatergic synapse, and presynaptic membrane (Fig. 4). The analysis results indicated the presence of potential targets in inflammatory response processes, cell cycle, and other biological functional processes. All of these targets are intricately linked to the onset and progression of OA, implying that multiple biological processes are involved in the treatment of OA with *O. corniculata* L. decoction.

KEGG pathway enrichment analysis was conducted on 190 potential targets employing the “Cluster Profiler” package in R language, yielding 106 signaling pathways ( $q$ -value < 0.05). These pathways were primarily involved in Chemical carcinogenesis-receptor activation, AGE-RAGE signaling pathway in diabetic complications, bladder cancer, prostate cancer, neuroactive ligand-receptor interaction, gastric cancer, proteoglycans in cancer, lipid and atherosclerosis, cellular senescence, and IL-17 signaling pathway. Ultimately, the enrichment results were visualized (Fig. 5).

### 3.4. Construction of the “*Oxalis corniculata* L. decoction-OA” network

The topological parameters of the network were assessed by utilizing the Network Analyzer plugin. The analysis results suggested an average neighboring node number of 4.789, network heterogeneity of 2.820, network density of 0.022, and network centrality of 0.861. The nodes with higher network neutrality value (degree) were considered the core nodes of the network, and the top 5 compounds ranked by degree were guanosine (degree = 39), 3-methyladipic acid (degree = 31), naringenin-7-O-beta-D-glucuronide (degree = 27), noroxxyhydrastinine (degree = 27), and chrysophanol 8-O-glucoside (degree = 26)

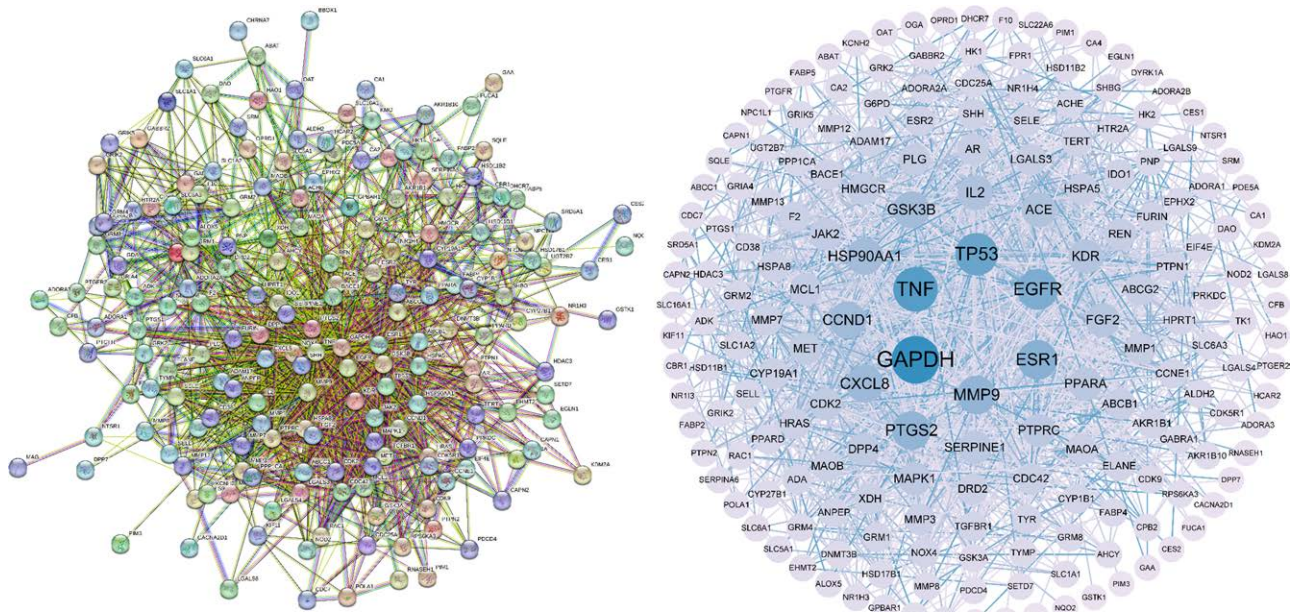


Figure 3. PPI network. PPI = protein–protein interaction.

**Table 2**  
Analysis of topological parameters of the top 10 core targets.

Gene	Degree	Betweenness centrality	Closeness centrality
GAPDH	104	0.163821	0.682482
TNF	89	0.098292	0.642612
TP53	80	0.079652	0.605178
EGFR	71	0.060238	0.601286
ESR1	66	0.047180	0.588050
PTGS2	61	0.040833	0.584375
MMP9	61	0.020028	0.566667
CXCL8	56	0.040016	0.561562
CCND1	54	0.019336	0.548387
GSK3B	53	0.024650	0.563253

(Table 3). Eventually, a comprehensive network model of “drug ingredient–target–pathway” was established utilizing Cytoscape 3.9.0 in Figure 6.

### 3.5. Molecular docking

The interaction strength of the target protein with the active ingredient was represented by the docking score. A binding energy below 0 signifies the ability of the drug ingredient to bind spontaneously to the target protein, whereas a binding energy below -5 kcal/mol signifies a moderate binding ability, and a binding energy below -7.0 kcal/mol signifies a strong binding ability.<sup>[9]</sup> The heat map of molecular docking is presented in Figure 7. Specifically, 21 combinations had binding energies below -5 kcal/mol, signifying moderate binding activity. Six combinations had binding energies below -7.0 kcal/mol, representing strong binding activity. Among them, the strongest binding ability was observed between naringenin-7-O-beta-D-glucuronide and EGFR.

The docking conformations for core component–target combination with the highest binding energy were visualized (Fig. 8). Guanosine formed hydrogen bonds with EGFR via CYS A:775, THR A:854, ASP A:855, and MET A:766 with a binding energy of -7.03 kcal/mol, indicating a strong binding ability. Additionally, 3-methyladipic acid formed hydrogen

bonds with EGFR via ASP A:855 with a binding energy of -5.59 kcal/mol, indicating a moderate binding ability. Naringenin-7-O-beta-D-glucuronide formed hydrogen bonds with EGFR via ASN A:842, ALA A:722, ARG A:841, and CYS A:775 with a binding energy of -8.26 kcal/mol. This indicates the strong binding ability of both. Moreover, noroxyhydrastinine formed hydrogen bonds with EGFR via LEU A:788 with a binding energy of -5.48 kcal/mol, indicating good binding interactions of small molecules with receptor proteins. Moreover, chrysophanol 8-O-glucoside formed hydrogen bonds with EGFR via ALA A:722, ASN A:842, LYS A:745, and ASP A:800 with a binding energy of -7.61 kcal/mol, indicating a strong binding ability.

### 4. Discussion

OA is an aging-related and injury-induced joint disorder characterized by degeneration of articular cartilage, osteosclerosis, and persistent low-grade inflammation.<sup>[10]</sup> China, being one of the world’s most populous nations, is undergoing a rapid aging process. Hence, OA will become one of the major concerns in the Chinese health system.<sup>[11]</sup> Traditional Chinese medicine has been widely utilized in treating fractures, osteoporosis, and other orthopedic-related diseases with good therapeutic effects due to its limited side effects and multiple targets.<sup>[12]</sup> In the present study, 539 compounds, mostly flavonoids, organooxygen compounds, and prenyl lipids, were identified from the *O. corniculata* L. decoction utilizing the UHPLC-Q-Exactive-MS/MS technique. The top 30 compounds were primarily flavonoids and carboxylic acids and their derivatives. The correlation analysis between the chemical constituents of the decoction and OA-related targets unveiled potential active ingredients for treating OA, such as guanosine, naringenin-7-O-beta-D-glucuronide, noroxyhydrastinine, and chrysophanol 8-O-glucoside. Guanosine, a raw material for the synthesis of cGMP, is crucially involved in the NO-cGMP signaling pathway regulation and enhances osteoblast proliferation, differentiation, and survival.<sup>[13]</sup> Naringenin-7-O-beta-D-glucuronide is a flavonoid and one of the metabolites derived from naringenin.<sup>[14]</sup> Naringenin-7-O-beta-D-glucuronide possesses multiple pharmacological properties such as antioxidant,

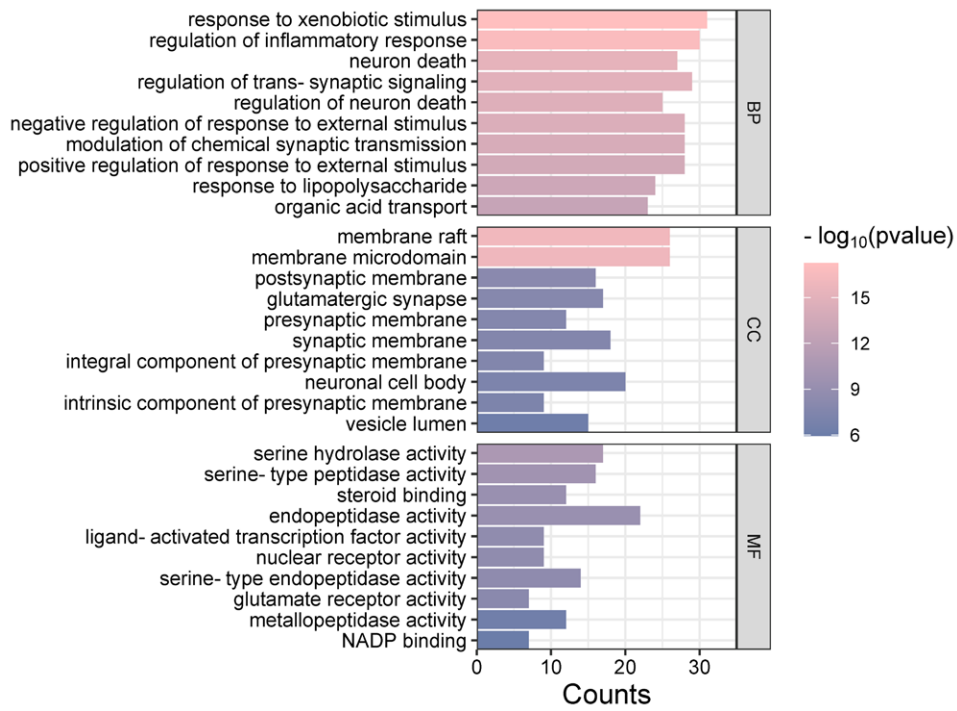


Figure 4. GO functional enrichment analysis. GO = gene ontology.

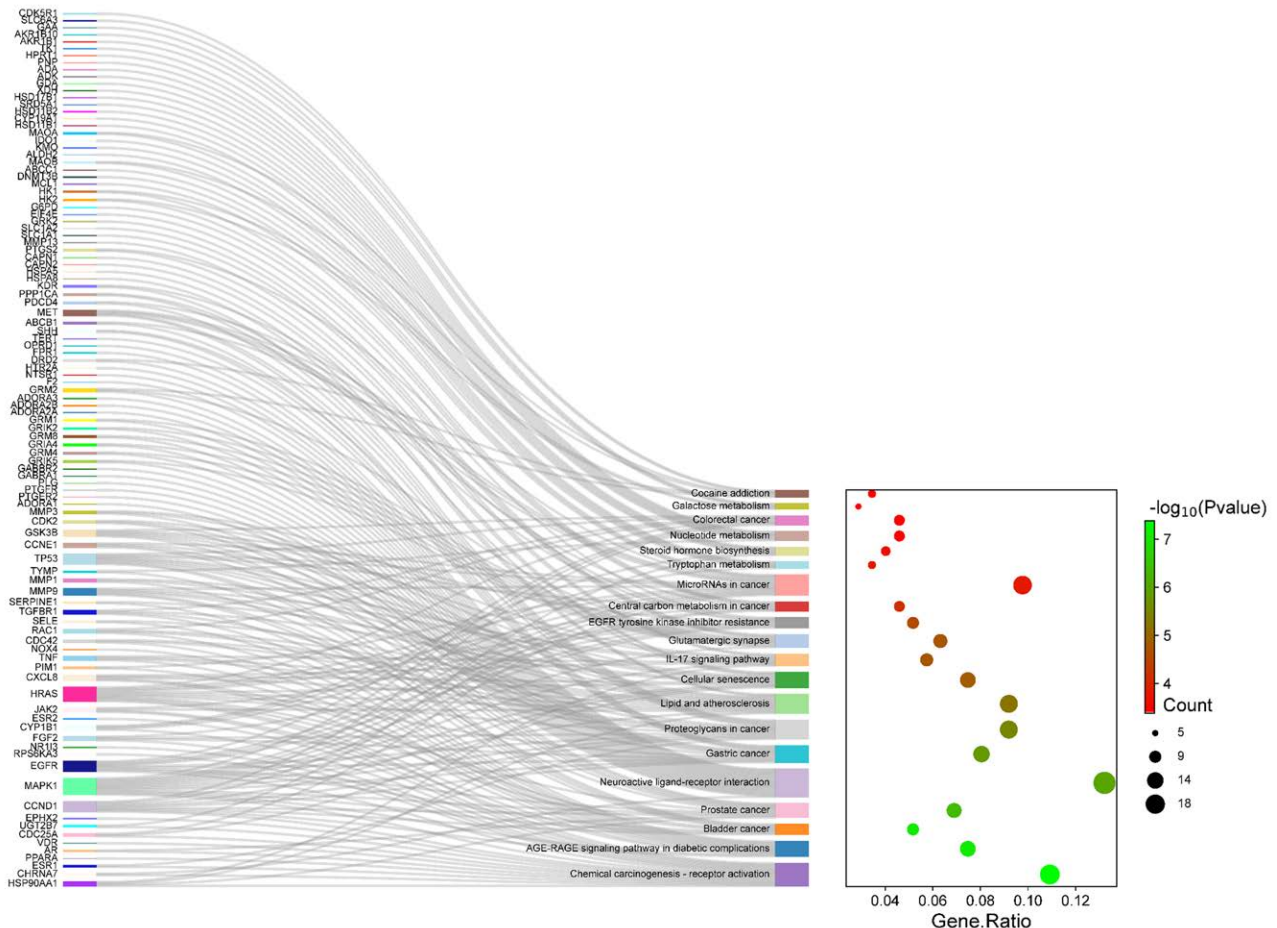


Figure 5. KEGG enrichment analysis. KEGG = Kyoto Encyclopedia of Genes and Genomes.

**Table 3**

**Top 10 compounds of *Oxalis corniculata* L. decoction in treating OA.**

Compound	Degree	Betweenness centrality	Closeness centrality
Guanosine	39	0.019124	0.382042
3-Methyladipic acid	31	0.011149	0.366554
Naringenin-7-O-beta-D-glucuronide	27	0.012588	0.374138
Noroxyhydrastinine	27	0.008638	0.361667
Chrysophanol 8-O-glucoside	26	0.008035	0.361667
2-Oxo-3-phenylpropanoic acid	17	0.0035365	0.351133
D-Leucine	17	0.003120	0.350000
Kaempferol 3-glucoside 7-rhamnoside	17	0.004192	0.361667
myo-Inositol	15	0.002433	0.345541
Panasenoside	15	0.003116	0.356908

OA = osteoarthritis.

anti-inflammatory, anticancer, antimicrobial, and cholesterol level-lowering.<sup>[15]</sup> Noroxyhydrastinine is an alkaloid with anti-inflammatory activity.<sup>[16]</sup> Chrysophanol 8-O-glucoside is a conjugated anthraquinone glycoside formed by combining chrysophanol with glucose. Conjugated anthraquinone glycoside exhibits pharmacological properties, including antibacterial,<sup>[17]</sup> anti-inflammatory,<sup>[18]</sup> and cancer cell inhibition.<sup>[19]</sup> The above-mentioned compounds exert pharmacological effects primarily by promoting cellular proliferation, differentiation, and anti-inflammation.

The PPI network analysis demonstrated that GAPDH, TNF, TP53, EGFR, and ESR1 possessed the highest node degree values, indicating their centrality within the network and their association with a substantial number of compound components. Therefore, these may be potential core targets of *O. corniculata* L. decoction in treating OA. GAPDH, a key enzyme in glycolysis, promotes cell proliferation and regulates apoptosis.<sup>[20]</sup> TNF, a member of TNF superfamily, encodes a multifunctional pro-inflammatory cytokine and has been associated with a wide range of disorders comprising insulin resistance, autoimmune diseases, psoriasis, and rheumatoid arthritis.<sup>[21]</sup> TP53, a

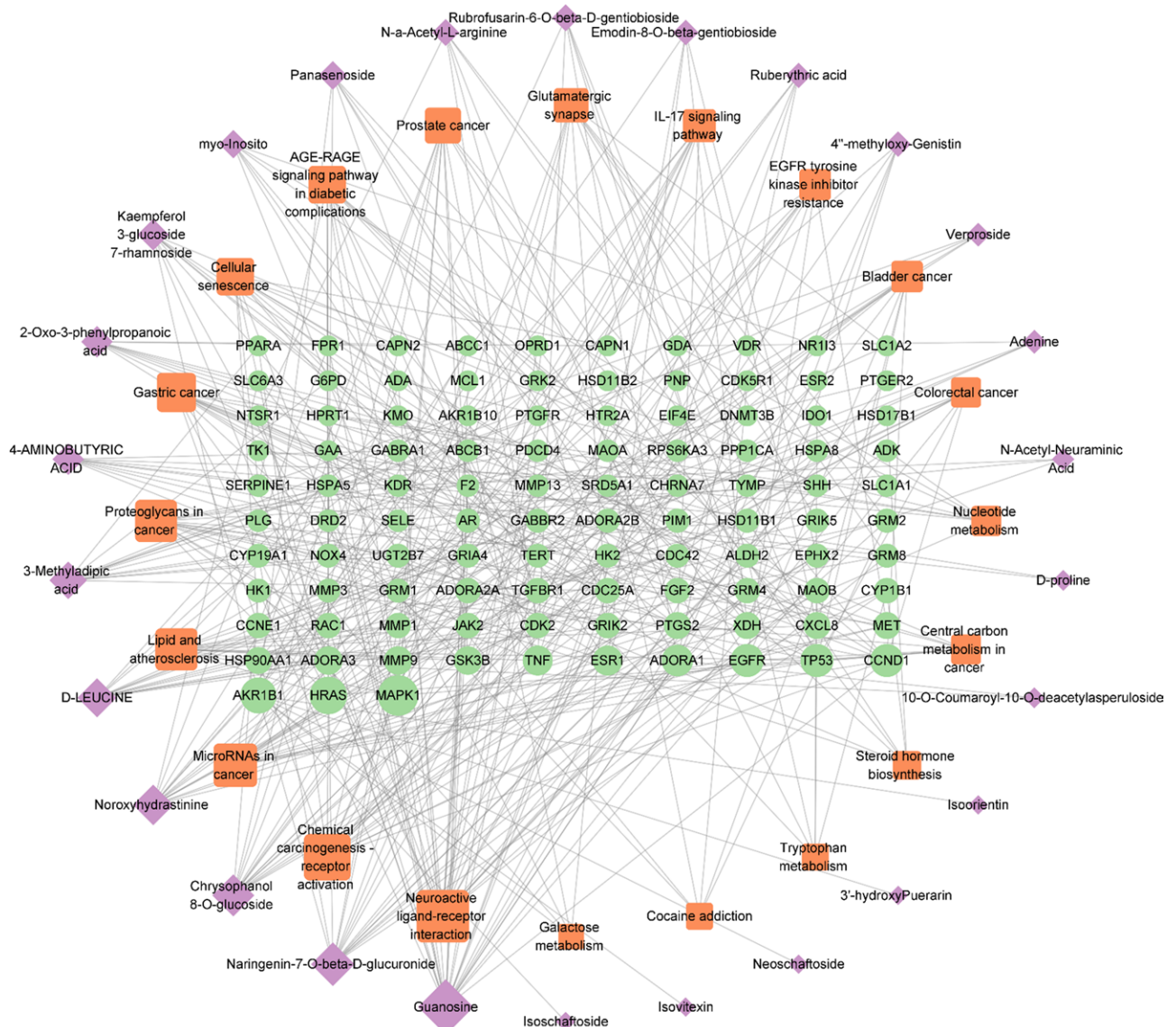


**Figure 6.** Network of “drug ingredient-target-pathway.” Green circles represent targets, purple diamonds represent drug components, and orange squares represent pathways.

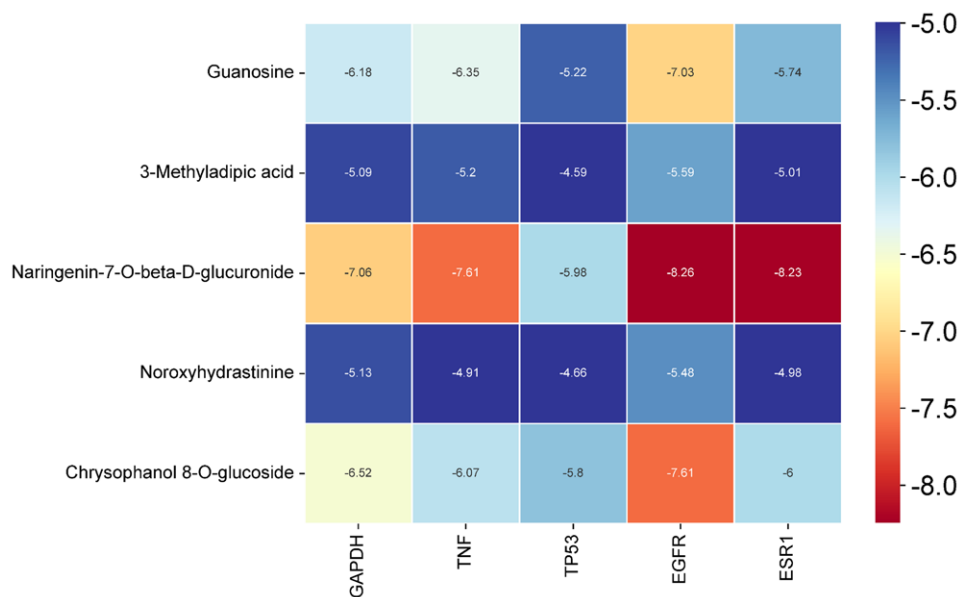


Figure 7. Composition-target binding energy heat map.

tumor suppressor gene, is critically involved in the inhibition of bone and soft tissue sarcomas progression.<sup>[22]</sup> EGFR, belonging to the ERBB family of tyrosine kinase receptors, regulates the proliferation and differentiation of osteoblasts, chondrocytes, and osteoclasts and plays an important role in bone biology and pathology.<sup>[23]</sup> ESR1, an estrogen receptor, is involved in bone metabolism and influences skeletal muscle formation.<sup>[24]</sup> Based on the above results, *O corniculata* L. decoction may regulate osteoblast proliferation and apoptosis by interacting with the mentioned targets, thereby offering a potential therapeutic approach for OA.

GO and KEGG enrichment analyses were conducted on 190 potential targets to predict the mechanism by which *O corniculata* L. decoction is involved in treating OA. GO analysis highlighted that the active ingredients of *O corniculata* L. decoction were involved in biological processes, including response to xenobiotic stimulus, regulation of inflammatory response, neuron death, regulation of trans-synaptic signaling, and regulation of neuron death. KEGG enrichment analysis indicated that the potential targets were primarily involved in signaling pathways, including lipid and atherosclerosis, cellular senescence, IL-17 signaling pathway, and EGFR tyrosine kinase inhibitor resistance. The lipid and atherosclerosis pathway is closely related to chronic inflammation, with associated inflammatory responses from the pathological stage, in which cholesterol, fatty acids, and modified lipids are capable of directly activating the inflammatory pathways.<sup>[25]</sup> In this study, the lipid and atherosclerosis pathway involved 16 targets, including MAPK1, TP53, and TNF, which were associated with inflammatory response. The target genes of IL-17 are generally antimicrobial molecules and cytokines.<sup>[26]</sup> IL-17 has beneficial effects at both local and systemic levels, and IL-17 in skeletal muscles affects several symptoms, such as muscle contractility defects and weakness.<sup>[27]</sup> In the present study, the IL-17 pathway primarily involved 10 targets, such as HSP90AA1, PTGS2, and CXCL8, which have significant effects on tissue repair, host defense, pathogenesis of inflammatory diseases, and cancer development. EGFR, which is a transmembrane tyrosine kinase, binds to EGF family ligands, activating several downstream signaling pathways, including MAPK, and promotes DNA synthesis and cell proliferation.<sup>[28]</sup> Cellular senescence, induced by various stresses, is associated with activation of antiapoptotic pathways and secretion

of pro-inflammatory and senescence-related substances.<sup>[29]</sup> Recognizing cellular senescence is an effective therapeutic idea to alleviate numerous chronic aging diseases, including osteoporosis. The findings of this investigation highlighted that the active ingredients in the *O corniculata* L. decoction act on OA through multi-targets and multi-pathways. However, there are some limitations to this study. In forthcoming research, pertinent pharmacological experiments will be conducted to substantiate these findings, thus providing a scientific groundwork for the development and application of *O corniculata* L. herbs.

## 5. Conclusion

In this study, the chemical constituents of *O corniculata* L. decoction were preliminarily identified utilizing the UHPLC-Q-Exactive-MS/MS technique. In addition, the core targets and components were simulated and validated by network pharmacology combined with molecular docking technique. Furthermore, the active components, core targets, and associated signaling pathways of *O corniculata* L. decoction in treating OA were analyzed. In summary, the outcomes of this investigation highlighted the potential anti-inflammatory properties of *O corniculata* L. decoction and its ability to promote osteoblast proliferation and differentiation, thereby offering novel insights into the processing of *O corniculata* L. herbs and the development of related drugs.

## Acknowledgments

We thank Bullet Edits Limited for the linguistic editing and proofreading of the manuscript.

## Author contributions

**Data curation:** Jian Zhang, Wanyan Shen, Hehe He.

**Funding acquisition:** Jian Zhang.

**Methodology:** Wanyan Shen.

**Supervision:** Hehe He.

**Writing – original draft:** Jian Zhang.

**Writing – review & editing:** Jian Zhang.



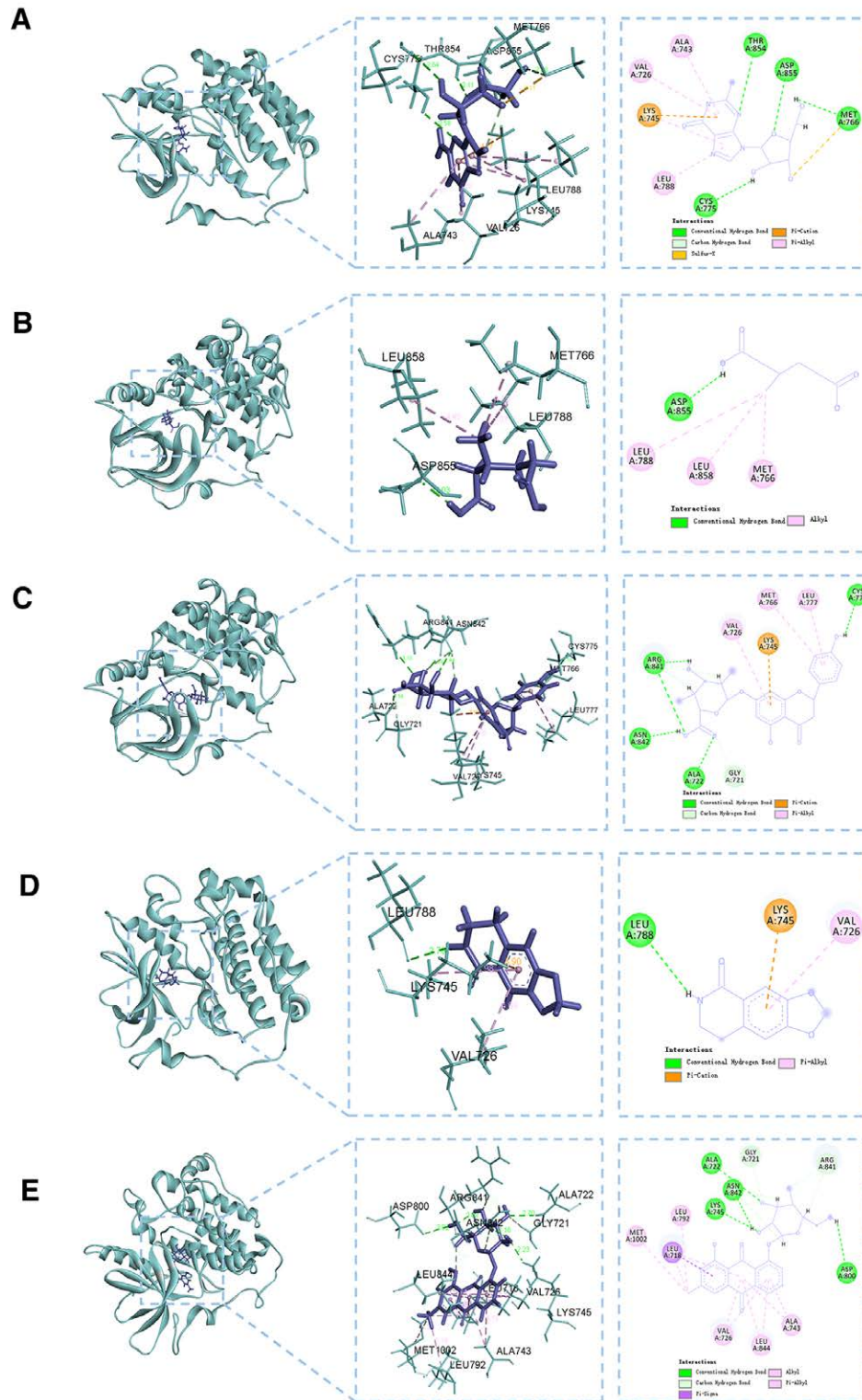


**Figure 8.** Molecular docking diagram. (A) Guanosine—EGFR; (B) 3-methyladipic acid—EGFR; (C) naringenin-7-O-beta-D-glucuronide—EGFR; (D) noroxyhydrastinine—EGFR; (E) chrysophanol 8-O-glucoside—EGFR. EGFR = epidermal growth factor receptor.

**References**

[1] Groom QJ, Van der Straeten J, Hoste I. The origin of *Oxalis corniculata* L. PeerJ. 2019;7:e6384.  
 [2] Gholipour AR, Jafari L, Ramezani M, et al. Apoptosis effects of *Oxalis corniculata* L. extract on human MCF-7 breast cancer cell line. Galen Med J. 2022;11:e2484.  
 [3] Guizhou Medical Products Administration. Quality Standards of Traditional Chinese Medicine and Ethnic Medicine in Guizhou Province. Guiyang, China: Guizhou Science and Technology Press; 2003:366.  
 [4] Yao Q, Wu X, Tao C, et al. Osteoarthritis: pathogenic signaling pathways and therapeutic targets. Signal Transduct Target Ther. 2023;8:56.

- [5] Liu T, Yao M, Zhao Y, Zhao S, Rui C, Yang F. Chinese medicine Gushukang capsule for treating primary osteoporosis: a systematic review and meta-analysis. *J Orthop Surg Res.* 2023;18:845.
- [6] Liu XY, Dong L, Liu, et al. Effect of *Oxalis corniculata* on cell proliferation and differentiation in human osteoblast-like SaOS-2 Cells (in Chinese). *Chin J Exp Tradit Med Formulae.* 2015;21:117–20.
- [7] Tang YT, Yang J, Li J, et al. Effects of *Oxalis corniculata* and musa basjoo sieb of gukangcapsule on fracture healing in rabbits and its mechanism (in Chinese). *J Guizhou Med UNIV.* 2022;47:635–9.
- [8] Liu J, Liu J, Tong X, et al. Network pharmacology prediction and molecular docking-based strategy to discover the potential pharmacological mechanism of Huai Hua San against ulcerative colitis. *Drug Des Devel Ther.* 2021;15:3255–76.
- [9] Hsin KY, Ghosh S, Kitano H. Combining machine learning systems and multiple docking simulation packages to improve docking prediction reliability for network pharmacology. *PLoS One.* 2013;8:e83922.
- [10] Xie C, Chen Q. Adipokines: new therapeutic target for osteoarthritis? *Curr Rheumatol Rep.* 2019;21:71.
- [11] Liu Q, Wang S, Lin J, Zhang Y. The burden for knee osteoarthritis among Chinese elderly: estimates from a nationally representative study. *Osteoarthritis Cartilage.* 2018;26:1636–42.
- [12] Tong X, Wang Y, Dong B, et al. Effects of genus epimedium in the treatment of osteoarthritis and relevant signaling pathways. *Chin Med.* 2023;18:92.
- [13] Kalyanaraman H, Schall N, Pilz RB. Nitric oxide and cyclic GMP functions in bone. *Nitric Oxide.* 2018;76:62–70.
- [14] Dall'Asta M, Derlindati E, Curella V, et al. Effects of naringenin and its phase II metabolites on in vitro human macrophage gene expression. *Int J Food Sci Nutr.* 2013;64:843–9.
- [15] Akamo AJ, Rotimi SO, Akinloye DI, et al. Naringin prevents cyclophosphamide-induced hepatotoxicity in rats by attenuating oxidative stress, fibrosis, and inflammation. *Food Chem Toxicol.* 2021;153:112266.
- [16] Liu L, Cui ZX, Yang XW, et al. Simultaneous characterisation of multiple *Mahonia fortunei* bioactive compounds in rat plasma by UPLC-MS/MS for application in pharmacokinetic studies and anti-inflammatory activity in vitro. *J Pharm Biomed Anal.* 2020;179:113013.
- [17] Janeczko M, Maslyk M, Kubiński K, Golczyk H. Emodin, a natural inhibitor of protein kinase CK2, suppresses growth, hyphal development, and biofilm formation of *Candida albicans*. *Yeast.* 2017;34:253–65.
- [18] Semwal RB, Semwal DK, Combrinck S, Viljoen A. Emodin – a natural anthraquinone derivative with diverse pharmacological activities. *Phytochem.* 2021;190:112854.
- [19] Wang T, Lu Z, Qu XH, et al. Chrysophanol-8-O-glucoside protects mice against acute liver injury by inhibiting autophagy in hepatic stellate cells and inflammatory response in liver-resident macrophages. *Front Pharmacol.* 2022;13:951521.
- [20] Cornett K, Puderbaugh A, Back O, Craven R. GAPDH in neuroblastoma: functions in metabolism and survival. *Front Oncol.* 2022;12:979683.
- [21] Fischer R, Kontermann RE, Pfizenmaier K. Selective targeting of TNF receptors as a novel therapeutic approach. *Front Cell Dev Biol.* 2020;8:401.
- [22] Thoenen E, Curl A, Iwakuma T. TP53 in bone and soft tissue sarcomas. *Pharmacol Ther.* 2019;202:149–64.
- [23] Schneider MR, Sibilio M, Erben RG. The EGFR network in bone biology and pathology. *Trends Endocrinol Metab.* 2009;20:517–24.
- [24] Pelusi L, Mandatori D, Di Pietrantonio N, et al. Estrogen receptor 1 (ESR1) and the Wnt/ $\beta$ -catenin pathway mediate the effect of the coumarin derivative umbelliferon on bone mineralization. *Nutrients.* 2022;14:3209.
- [25] van Diepen JA, Berbée JF, Havekes LM, Rensen PC. Interactions between inflammation and lipid metabolism: relevance for efficacy of anti-inflammatory drugs in the treatment of atherosclerosis. *Atherosclerosis.* 2013;228:306–15.
- [26] Wilson SC, Caveney NA, Yen M, et al. Organizing structural principles of the IL-17 ligand-receptor axis. *Nature.* 2022;609:622–9.
- [27] Amatya N, Garg AV, Gaffen SL. IL-17 signaling: the Yin and the Yang. *Trends Immunol.* 2017;38:310–22.
- [28] Huang LH, Fu LW. Mechanisms of resistance to EGFR tyrosine kinase inhibitors. *Acta Pharmaceutica Sinica B.* 2015;5:390–401.
- [29] Farr JN, Khosla S. Cellular senescence in bone. *Bone.* 2019;121:121–33.